Wei, Chu-liang and Lai, Chun-cheung and Liu, Shun-yee and Chung, W.H. and Ho, Tin Kin and Tam, Hwa-Yaw and Ho, S.L. and McCusker, A. and Kam, J. and Lee, K.Y. (2010) ***A fiber Bragg grating sensor system for train axle counting.*** IEEE Sensors Journal, 10(12). pp. 1905-1912.

A Fiber Bragg Grating Sensor System for Train Axle Counting

Chu-liang Wei, Chun-cheung Lai, Shun-yee Liu, W. H. Chung, T. K. Ho, Hwa-yaw Tam, S. L. Ho, A. McCusker, J. Kam, and K. Y. Lee

***Abstract*—Railway signaling facilitates two main functions, namely, train detection and train control, in order to maintain safe separations among the trains. Track circuits are the most commonly used train detection means with the simple open/close circuit principles; and subsequent adoption of axle counters further allows the detection of trains under adverse track conditions. However, with electrification and power electronics traction drive systems, aggravated by the electromagnetic interference in the vicinity of the signaling system, railway engineers often find unstable or even faulty operations of track circuits and axle counting systems, which inevitably jeopardizes the safe operation of trains. A new means of train detection, which is completely free from electromagnetic interference, is therefore required for the modern railway signaling system. This paper presents a novel optical fiber sensor signaling system. The sensor operation, field setup, axle detection solution set, and test results of an installation in a trial system on a busy suburban railway line are given.**

***Index Terms*—Axle counting, fiber Bragg grating (FBG), remote sensing, train detection.**

I. INTRODUCTION

WITH THE high-speed operation and tight headway requirement in modern railways, a fail-safe signaling system is vitally important to ensure the provision of safe and reliable railway services. In order to maintain adequate separation among the trains, train detection to identify the presence, or otherwise, of the train in front within a particular section of track; and speed control on the train behind to regulate its movement according to the location of the train in front, are the two main functions of signaling systems. Based on the underlying principles of the traditional fixed-block signaling, track circuits and axle counters have been widely used as the train detection means in practice.

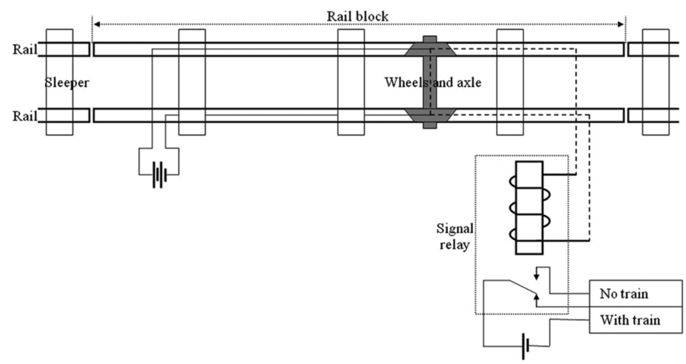

Fig. 1. Operation principle of track circuit.

Track circuit refers to a complete electrical circuit with a power source at one end of a section of track (often termed as a signaling block), the rails, and a receiver (in its primitive form, a relay) at the other end [1], [2]. When the signal reaches the receiver, it confirms the complete circuit, which is thus in the 'energized' state. When a train is present within the block, the train wheels shunt the track circuit and the receiver is de-energized. The operation is fail-safe as any disruption or malfunction with the track circuit renders no signal being received by the receiver, thereby indicating the presence of a train. Fig. 1 illustrates the operation of a simple track circuit.

With the introduction of electrification in railways, the rails are often used to carry the traction return current. As a result, the track circuit and the traction circuit, which are of different level of power, share the rails as the common circuit component. To avoid interference, the power source of the track circuit usually adopts a different form from that of the traction supply. However, given the traction power feeding system and the power electronics traction drivers are sharing the same path and the former is much larger in magnitude compared to the latter, electromagnetic interference (EMI) is almost inevitable. Stringent requirements are specified nowadays to ensure electromagnetic compatibility (EMC) of the signaling system is fully addressed in the process of system integration and safety assurance. However, it is noted that even with EMC well safeguarded in practice, track circuits are still subject to operation failures in hostile environment, such as the areas susceptible to flooding.

Axle counters, on the other hand, do not rely on a physical closed electrical circuit. Each axle counter consists of literally a pair of electromagnetic coils mounted on either side of the rail head as shown in Fig. 2, one being the transmitter and the other the receiver. A magnetic field is established between the two coils. When a train wheel is running on the rail and between the

Manuscript received November 17, 2009; revised February 27, 2010; accepted April 12, 2010. Date of publication June 07, 2010; date of current version October 13, 2010. This work was supported by the Hong Kong Polytechnic University and Shantou University. The associate editor coordinating the review of this paper and approving for publication was Prof. Evgeny Katz.

C. Wei is with the Department of Electronic Engineering, Shantou University, Shantou, Guangdong 515063, China (e-mail: chuliangwei@hotmail.com).

C. Lai, S. Liu, W. H. Chung, T. K. Ho, H. Tam, and S. L. Ho are with the Department of Electrical Engineering, Hong Kong Polytechnic University, Kowloon, Hong Kong (e-mail: bskenlai@inet.polyu.edu.hk; eesyliu@inet.polyu.edu.hk; eewhchun@polyu.edu.hk; eetkho@polyu.edu.hk; eehytam@polyu.edu.hk; eeslho@polyu.edu.hk).

A. McCusker, J. Kam, and K. Y. Lee are with the MTR Corporation, Ltd., Kowloon, Hong Kong (e-mail: mccusker@mtr.com.hk; jkam@mtr.com.hk; tkyylee@mtr.com.hk).

Color versions of one or more of the figures in this paper are available online at http://ieeexplore.ieee.org.

Digital Object Identifier 10.1109/JSEN.2010.2049199

Fig. 2. Axle counter consists of two pairs of transmitter and receiver. Inset shows the track side converter equipment connecting the axle counter.

coils, the magnetic field is so distorted that the induced voltage on the receiving coil changes direction, which registers the passage of one wheel. Two sets of axle counters are installed at the two ends of a signaling block; and a comparison of wheel passage count of the two axle counters verifies whether there is train occupancy in the block (when the axle counts of the two counters are different) or whether the train has moved away from the block (when the axle counts of the two counters are the same) [3], [4]. However, as the operation hinges on the delicate changes of magnetic field, EMI remains to be a genuine concern for the reliable operation of axle counters.

This study proposes an innovative and EMI-free approach of axle counting, a fiber Bragg grating (FBG) sensor system, for the detection of train wheel passage. The purpose of the proposed system is to enhance the accuracy and reliability of train detection and hence provide the signaling system with better safety assurance.

II. FBG Sensors

A. The Principle

A FBG sensor is an in-fiber reflector which reflects light centered at the Bragg grating wavelength, λ_B, which is given by [5]

$$\lambda_B = 2n\Lambda \tag{1}$$

where n is the effective refractive index of the fiber core and Λ is the period of the index modulation. The wavelength shift $\Delta\lambda_B$ with respect to changes in axial strain $\Delta\varepsilon$ and temperature ΔT is given by the following relation [6]:

$$\frac{\Delta\lambda_B}{\lambda_B} = (1-\rho_\varepsilon)\Delta\varepsilon + (\alpha+\zeta)\Delta T \tag{2}$$

where ρ_ε is the photoelastic coefficient of the fiber, α is the thermal expansion coefficient of the fiber material, and ζ is the thermooptic coefficient of the fiber material. For 1.5 μm FBG sensors fabricated in silica fiber, the wavelength-strain and wavelength-temperature sensitivities are $\sim$ 1 pm/$\mu\varepsilon$ and $\sim$ 13 pm/°C, respectively.

B. Sensor Fabrication and Interrogator

An ultraviolet (UV) laser is used to inscribe FBG sensor through a phase mask into single-mode fibers. The reflected wavelength depends on the Λ of the phase mask and the UV-induced refractive index of the fiber. Typical length of a FBG sensor is about 10 mm.

In order to acquire the FBG sensor signal, an interrogator is used to launch light into the optical fiber with FBG sensors (with different λ_B) and collect the reflected light back for analysis. The block diagram of the interrogator is shown in Fig. 3. The wavelengths of the reflected light are measured and then transmitted to a signal processing unit for analysis and data log. An interrogator can interrogate about 40 to 80 FBG sensors for each channel (for an interrogator with wavelength range of 80 nm and each FBG occupies 1–2 nm operation bandwidth). By using FBG sensor with a bandwidth of 0.25 nm, the long-term wavelength measurement stability and repeatability of the interrogator are 2 and 1 pm, respectively, while the dynamic range (the laser launch power minus the detection noise floor) of the interrogator is 25 dB, tens of km of optical fiber (loss of ~0.2 dB/km) can, therefore, be used to link up the FBGs without affecting the measurement accuracy. The maximum refresh rate of a commercially available interrogator on each sensor is up to 2 kHz, while the one used in this study is 250 Hz.

C. Applications

FBG sensors have been widely used to measure temperature and strain in various engineering applications, such as oil refineries and civil infrastructures, because of their electromagnetic immunity, low loss, and multiplexing capability [6]–[8]. Moreover, coupled with suitable transducers, the FBG sensors can also be employed to measure other parameters, such as pressure, and displacement.

FBG sensors have also been increasingly employed in the railway industry in recent years. Successful applications of FBG sensors for train speed measurement, train load estimation, derailment detection, wheel-defect detection, rail crack detection, strain monitoring of train structures and bogie health monitoring have been reported [9]–[12]. FBG sensing systems indeed have good potentials to become the future technology for railway applications.

III. Axle Counting by FBG Sensors

Axle counting by FBG sensors is based on measuring the strain changes in the rail upon the passage of trains at the measurement points. When a train is running on a measurement point, the rail in the vicinity is momentarily deformed, i.e., the rail head is in compression while the rail foot is in tension, due to the shear weight of the train. FBG sensors installed on rail therefore measure the strain change of the deformed rails. It is expected that a conspicuous and distinctive peak can be identified in the strain change signals measured by the FBG sensors when a train wheel is pressing on the rail in the vicinity of the measurement point.

A. Position of Sensor Installation

In order to ensure the most sensitive measurement of strain change on the rail and hence the most appropriate positions for installing the sensors, it is necessary to analyze the momentary

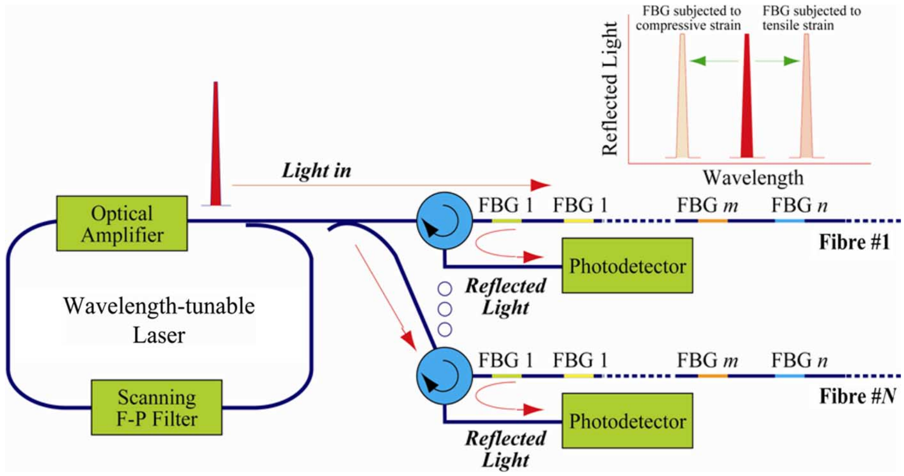

Fig. 3. Block diagram of a FBG interrogator.

deformation of the rail due to a passing wheel. The ANSYS Multiphysics software has been employed to simulate the levels of rail deformation when a train is standing by the rail. The rail model UIC54 is adopted in the simulation. It is made of steel, with a Young's modulus of 207 GPa and a Poisson ratio 0.29. Under the weight of a static train car of 48 tones, supported by eight wheels, the maximum deformation of the track is found at its head of the rail where the train wheel stands, and the second highest deformation is at the rail foot, as shown in Fig. 4(a). In the longitudinal direction, the deformation is gradually reduced away from the contact point. In the vertical direction, the rail web suffers from the least deformation, and both the rail head and foot are experiencing high deformation.

To further verify the findings of the simulation and to confirm the best positions for the installation of the FBG sensors, an experiment has been carried out in the laboratory to measure the strain change at various positions of the rail induced by passage of a test train.

The experiment setup is illustrated in Fig. 4(b). Seven FBG sensors are installed at different cross-section positions of a short section of rail, three of them are installed vertically, and the other four are installed longitudinally. The test train, which is seven tones in weight with a four-wheel bogie, is driven over the rail with a speed of about 5 km/h. Fig. 4(c) shows the result of measured strain signal of the seven sensors when the train passes the measurement point four times. Evidently, the longitudinal FBGs 1 and 4 record the highest compressive and tensile strain, respectively. The longitudinal FBG 3 and vertical FBG 5 experience the second and third largest strain, respectively. The vertical FBG 6 experiences the second highest compressive strain. The results are in good consistency with those of the simulation. It also highlights that the horizontally installed sensors allow more sensitive measurements than those offered by the vertically installed sensors.

To summarize, the best sensor installation position for measuring strain change on the rail is the head and foot of the rail, respectively. However, it is not practical to install FBG sensor on the head of the rail because of safety considerations. Thus, the position of FBG 4 is chosen for the field test.

B. Test Track Setup

In the field test, the system is employed to record the axle counts within a signaling block of MTR West Rail in Hong Kong, as shown in Fig. 5(a). The West Rail links the North-West New Territory (Tuen Mun) and the city center (Nam Cheong of Kowloon), and its length is 30.5 km with nine stations. Running on the West Rail, there are 22 set (seven cars per set) trains. The maximum speed of the trains is 130 km/h. The train length is 220 m, and its maximum capacity is 2345 persons. The power is supplied through overhead lines with 25 kV/50 Hz. Two types of track-forms: floating slab track (FST) for the viaduct sections, and low vibration track (LVT) for the tunnel sections, with UIC60 model track are currently used in the West Rail.

The block near the Tsuen Wan West station, named CB block, is chosen to test the FBG axle counting system. It includes two junctions and it is defined by five boundary points which are also the axle-counting points AH23, AH25, AH26, AH29, and AH30 of the existing axle-counter system, as shown in Fig. 5(b). The CB block is one of the typical axle counting blocks containing five entries in the West Rail. The sensors are installed in the three main (frequently used) measurement points of AH23, AH29, and AH30, and they are connected to an interrogator via 4 km of standard optical fiber cable. The interrogator and the controlling computer are located at the Signal Equipment Room of the Tsuen Wan West station. The lengths between entries AH23 and AH29, AH23, and AH30, and AH29 and AH30 are about 1500, 1200, and 600 m, respectively.

IV. Detection Methodologies Development

The data of strain variations at the measurement points have been logged for over six months. Fig. 6(a) shows typical strain change of a deformed rail when a train passes through the measurement point of the rail. The reflective wavelengths of the FBG sensors are in the range of 1535 to 1575 nm and the change of wavelength detected is within 0.3 nm which corresponds to a change of strain of 300 $\mu\varepsilon$. The 28 strain signal peaks in Fig. 6(a) clearly indicate the 28 axles of a seven-car train. From two consecutive peaks in the signal, together with the inter-axle length, the instantaneous train speed can also be derived.

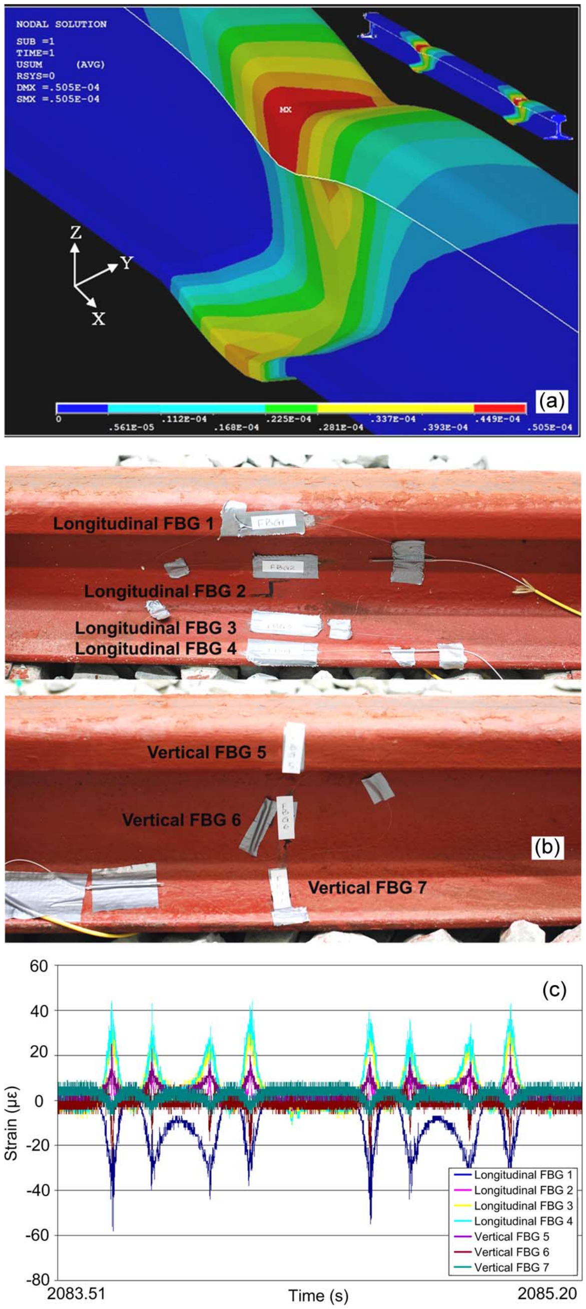

Fig. 4. (a) Simulation of strain profile of the rail when a train wheel is standing by the rail. (b) Upper photo shows the four longitudinal FBGs installed at one side of the rail and the lower shows the three vertical FBGs installed at the other side of the test. (c) Measured strain of the seven FBGs when the train passes the measurement point four times.

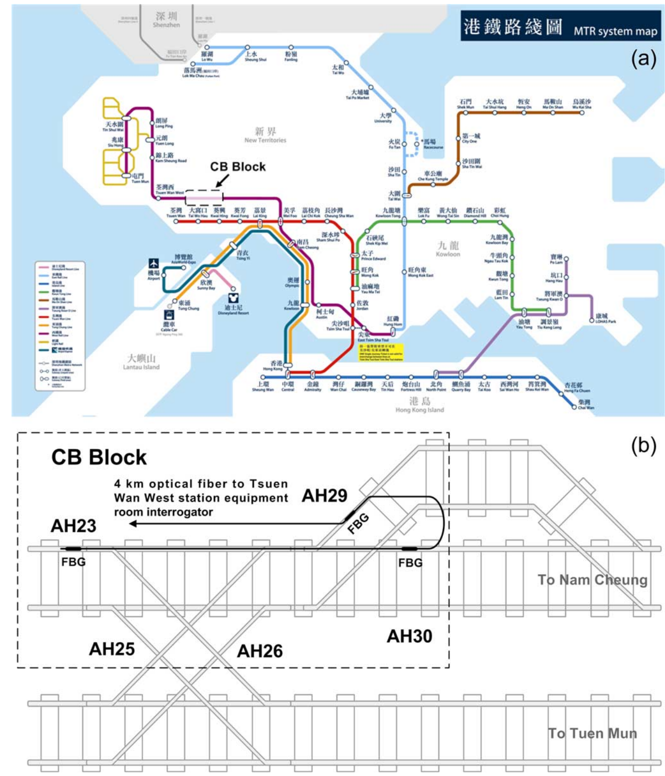

Fig. 5. (a) Route map of the MTR West Rail; the CB block for conducting the test is highlighted. (b) FBG sensors connection in the CB block.

In order to facilitate the purpose of axle detection, an automatic and intelligent software tool to count the signal peaks (which corresponds to the count of the axles) of a train is required. However, certain situations are making the identification of strain signal peaks difficult. For instance, Fig. 7(a) shows the strain change signal when a train just stops at the measurement point; and it also contains a noisy peak which is not as apparent as others. Therefore, a solution set of peak identification needs to be found in order to realize reliable axle counting.

Some noisy strain change signals, as shown in Fig. 6(b), are also making the peak identification difficult. To smoothen the signals for peak detection, the signals are first low-pass-filtered with a cutoff frequency of 10 Hz. Fig. 6(c) shows the filtered result of the raw signals, as shown in Fig. 6(b).

A. Initial Peak Identification: X-Crossing

This approach provides a preliminary detection of the signal peaks.

Description: To verify there is a peak in the signal, a rising edge, followed by a falling edge, has to be identified. A preset threshold is used for comparison to confirm there is a rising edge or a falling edge. In order to make allowances for the noisy peaks; and to screen off the unique signal pattern when a train stops at the measurement point, as shown in Fig. 7(a), a hysteresis threshold setting, i.e., two different thresholds to detect the rising edge and the falling edge, respectively, is employed.

Hysteresis Thresholds Setting: The strain signal waveform is mainly related to train weight and speed, and wheel and track condition. Different/irregular strain signal waveform makes the setting for suitable thresholds difficult. With this approach, the difference between the minimum value of the peaks and the maximum value of the troughs on the signals induced by different types of trains, including the electro-multiple-units (EMU) passenger train, locomotive, and permanent-way machines, is referred as X, and this value is taken into account when setting the values of the two thresholds. Based upon the experiment data obtained, it is found that the best cutoff values arise when the thresholds for detecting the rising edge and the falling one are, two-thirds and one-third of X, respectively.

Time Interval Setting: Even with the use of low-pass-filter, some noisy peaks still remain, as shown in Fig. 7(a), because of

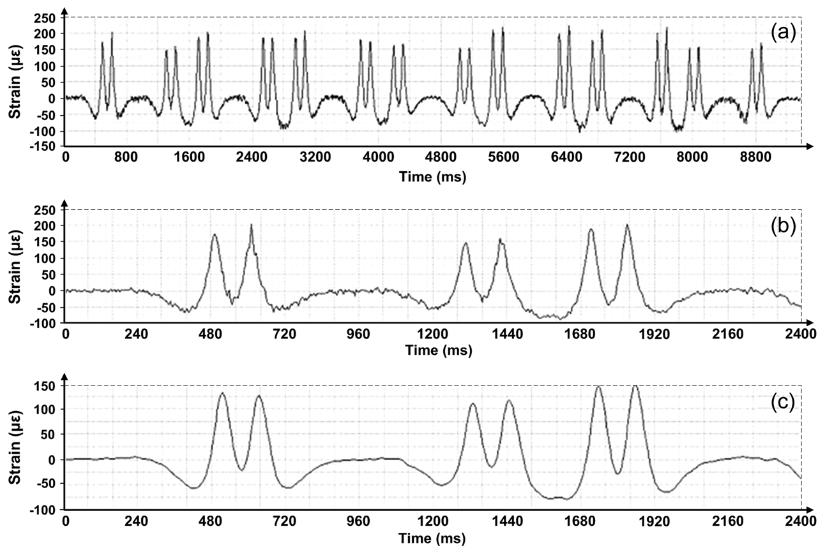

Fig. 6. Measured strain change (a) induced by a passage of a train with 28 wheels, (b) of the first six wheels, and (c) the low-pass-filtered result of the signal in (b).

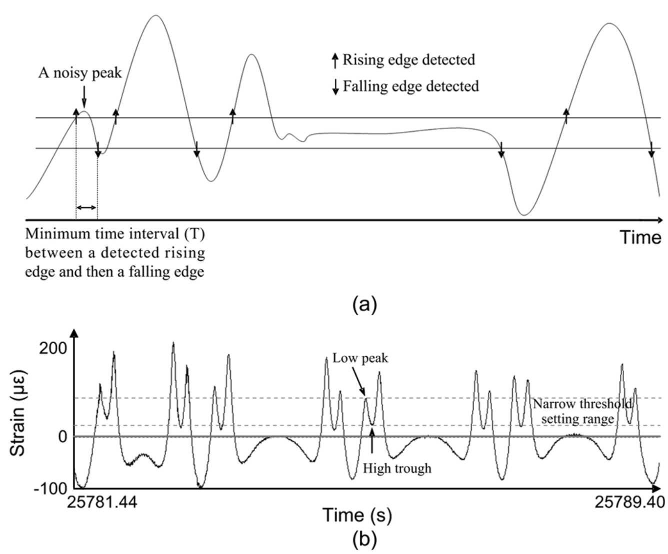

Fig. 7. (a) Illustration of the X-crossing method and the setting of minimum time interval and (b) the narrow range for threshold setting of this method.

poor condition of wheel and/or rail. To address such noisy peaks, the time interval between a detected rising edge followed by a falling edge is obtained and compared with a preset minimum time interval (T).

Based upon experiment results, a train wheel is detected (the rail of the measurement point is shortened) when it is away from the measurement point about 4.7 m, while the rail is lengthened (generating an axle peak) only when the train wheel is within about 1.1 m of the measurement point. The train speed of the measurement point is about 60–90 km/h, thus the duration of a signal peak induced by a normal train wheel is around 88–132 ms (i.e., 22–33 sampling points). However, from the experimental results, the duration of a noisy peak is less than 28 ms (i.e., seven sampling points) mostly. Thus, the T is set to 24 ms (i.e., six sampling points).

Results and Disadvantages: During the initial test (45 days), 9000 trains (252,000 axles) passed through the AH23 measurement point, and the numbers of axles of the trains have been detected correctly, with the exception of thirteen trains only.

All the thirteen trains with failed counts have found missing axle count. They include ten permanent-way machines and three passenger trains (likely to be the same train on different occasions). Fig. 7(b) illustrates the typical signals of one of the permanent-way machines. The threshold setting required to detect peaks in the signals of the 13 trains should have been much narrower (because the troughs of the signal waveform are much higher than those caused by most passenger trains; however, the peaks are much lower than those caused by most passenger trains). Moreover, the time intervals of some signal peaks incurred by these thirteen trains' wheels are around 40 ms (i.e., ten sampling points), with which the preset minimum time interval T cannot be achieved (e.g., the time interval between a detected rising edge followed by a falling edge of a peak with ten sampling points normally is 16 or 20 ms, that is less than the T), and hence some axles are missed in the counting process.

B. Further Improvement: D(erivative)-Crossing

To further improve the accuracy of peak detection, the D-crossing method is developed to supplement the X-crossing method as a solution set.

Description: The X-crossing method is not able to detect the peaks as shown in Fig. 7(b). The D-crossing method solves this drawback by using the first-derivative (Y_i) of the signal, given by (3), from the preceding signal point (x_{i-1}) and the next signal point (x_{i+1}), at a particular point of the signal, to detect a peak once a change in sign is discovered on the derivatives

$$Y_i = (x_{i+1} - x_{i-1})/2dt \tag{3}$$

where $i = 0, 1, 2 \ldots \mathrm{n} - 1$.

To avoid a local peak (at the valley between two bogies, as shown in Fig. 8(a)) is interpreted as the passage of a train wheel, this method sets a threshold to cutoff the lower part of the signal before it is used for peak detection. Fig. 8(c) shows the first derivative result of a signal.

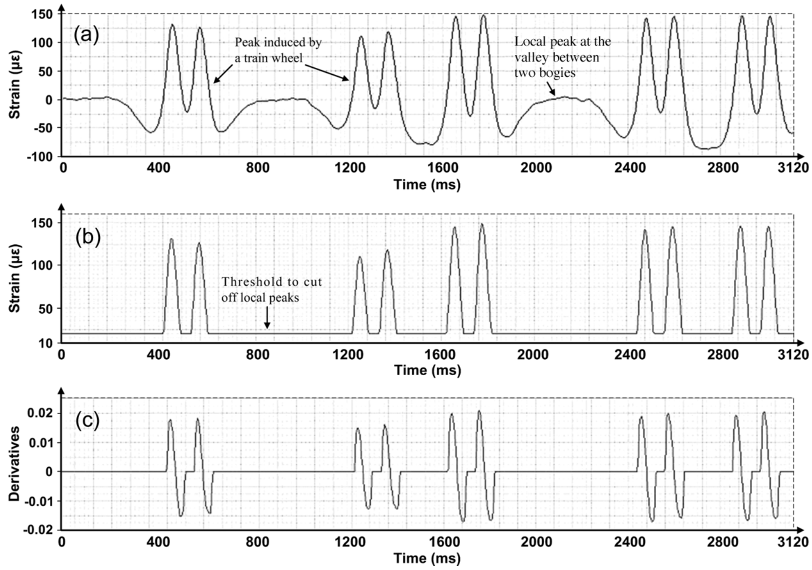

Fig. 8. Illustration of the D-crossing method. (a) Signal including the axle peaks induced by passage of train wheels, and the local peaks which are in-between two bogies. (b) Setting of threshold to cut off local peaks. (c) First derivatives of the signal in (b).

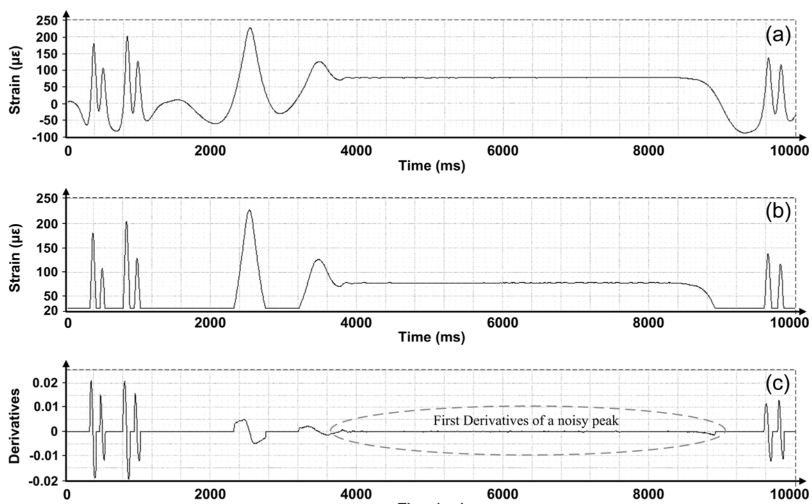

Fig. 9. Noisy peak in the captured signal when a train is stopped at the measurement point (a) the low-pass-filtered signal, (b) cutting off the local peak by threshold setting, and (c) first derivatives of the signal in (b).

This method needs at least four values of the derivative, including two positives and two negatives, to confirm an axle peak. To gain four values of the derivative, six signal points (i.e., $\text{time interval} = 24\ \text{ms}$) are needed. The number of data available for a noisy peak is normally less than six, thus the noisy peak, as shown in Fig. 7(a), can usually be filtered out.

Solution Set: To prove that the D-crossing method can identify the axle peaks which have been missed by the X-crossing method, the data of the 9000 trains were detected by the D-crossing method through computer simulation. The peaks of the 13 wrongly detected trains in the previous tests have been identified positively. However, there is still a train being incorrectly detected, as shown in Fig. 9, by the D-crossing method, because the noisy peak of the signal (captured when a train is stopped at the measurement point) consists of more than six sampling points (i.e. with a $\text{time interval} = 24\ \text{ms}$, it can produce four values of the derivative including two positives and two negatives). However, the train can be correctly detected by the X-crossing method. During the entire test period, no "phantom" axle was counted after using both methods. As a result, two methods are now employed together to form a solution set for the study, and the better results of any method are recorded.

Results: To verify the counting results of the system, the proposed system is operated as a shadow to the existing axle-counter system, and thus discrepancies between the two systems are apparent and hence the comparison result is very reliable.

During the test over five months, 30,008 (840,224 axles), 10 (280 axles), and 29,998 (839,944 axles) trains passed through the AH23, AH29, and AH30 measurement points, respectively. No train has been wrongly detected in any measurement point, therefore the success rate of axle counting of all the measurement points are 100%.

V. Conclusion

A FBG-sensors-based axle-counting system has been proposed and developed. The principles and application of the FBG sensors are described, followed by the field test setup. The test results of the system are given, together with the description of the development of the solution set for signal peak detection.

The 100% successful detection rate has shown that the system is a useful and effective alternative to the existing axle counting systems for trains within a particular zone of rail. The feasibility of employing EMI-free FBG sensors in train axle counting is well proven in this study. The system has been continuously tested for over six months. Neither the sensors installed at the track side nor interrogator housed in the equipment room has been found in any malfunction. Optical fiber is well proven to be operated over 25 years without performance degradation and the sensors installed in the field are well protected, we believe this remote-sensing system is able to provide reliable and accurate axle-counting function over a long period of time.

Railway operation requires very high safety integrity level train detection because human lives at stake. The preliminary test is not yet adequate to ensure the overall integrity of the proposed axle-counting system in real situations. Further tests are still needed in both the CB block and more complicated signaling blocks. To improve the accuracy and reliability of the system, the system can be further enhanced with the development of more intelligent peak identification algorithms; adoption of redundancy FBG sensor on each measurement point to assure high availability of measurement; and the development of FBG sensors with improved strain sensitivity.

Acknowledgment

The authors are grateful for technical support from the the MTR Corporation, Ltd., Hong Kong.

References

[1] N. Nedelchev, “Influence of earth connection on the operation of railway track circuits,” in *IEEE Proc. Electric Power Applications*, 1997, vol. 144, no. 3, pp. 215–219.

[2] T. Akio, “Development of a train detection system and a spread spectrum transmission system for track circuit,” in *Proc. IEEE Vehicular Tech. Conf.*, May 1997, vol. 3, pp. 1922–1926.

[3] I. Lucic, “Holistic safety performance forecasting for train detection system,” in *Proc. IEEE Int. Conf. System, Man, Cybern.*, Oct. 2005, vol. 3, pp. 2973–2978.

[4] P. R. Goundan and A. Jhunjhunwala, “Axle counter based block signaling for safe and efficient train operations,” in *Proc. IEEE Veh. Tech. Conf.*, Sep. 1999, vol. 2, pp. 824–828.

[5] A. Othonos and K. Kalli*, Fiber Bragg Gratings—Fundamentals and Applications in Telecommunications and Sensing*. Norwood, MA: Artech House, 1999, pp. 95–99.

[6] T. H. T. Chan, L. Yu, H. Y. Tam, Y. Q. Ni, S. Y. Liu, W. H. Chung, and L. K. Cheng, “Fiber Bragg grating sensors for structural health monitoring of Tsing Ma bridge: Background and experimental observation,” *Eng. Struct.*, vol. 28, no. 5, pp. 648–659, 2006.

[7] P. Ferdinand, S. Magne, V. Dewynter-Marty, C. Martinez, S. Rougeault, and M. Bugaud, “Applications of Bragg grating sensors,” in *Eur. Opt. Soc. Amer. Tech. Dig.*, 1997, vol. 16, pp. 14–19.

[8] Y. J. Rao, “Recent progress in applications of in-fiber Bragg grating sensors,” *Opt. Lasers Eng.*, vol. 31, no. 4, pp. 297–324, 1999.

[9] H. Y. Tam, S. Y. Liu, B. O. Guan, W. H. Chung, T. H. Chan, and L. K. Cheng, “Fiber Bragg grating sensors for structural and railway applications,” in *Proc. Photonics Asia 2004: Advanced Sens. Syst. Appl. II 5634*, Beijing, China, Apr. 2004, pp. 85–97.

[10] K. Y. Lee, K. K. Lee, and S. L. Ho, “Exploration of using FBG sensor for axle counter in railway engineering,” *WSEAS Trans. Syst.*, vol. 3, no. 6, pp. 2440–2447, Aug. 2004.

[11] K. Y. Lee, K. K. Lee, and S. L. Ho, “Exploration of using FBG sensor for derailment detector,” *WSEAS Trans. Syst.*, vol. 3, no. 6, pp. 2433–2439, Aug. 2004.

[12] H. Y. Tam, S. Y. Liu, W. H. Chung, T. K. Ho, S. L. Ho, and K. K. Lee, “Smart railway sensor network using fiber Bragg grating sensors as sensing elements,” in *Advanced Smart Materials and Smart Structures Tech.*. Daejeon, Korea: Techno-press, 2005, vol. 1, pp. 159–169.

Chu-liang Wei received the B.Sc. and Ph.D. degrees from the Department of Electrical Engineering and Electronics, University of Liverpool, Liverpool, U.K., in 2003 and 2006, respectively.

From 2007 to 2009, he was with the Department of Electrical Engineering, Hong Kong Polytechnic University. He then joined the Department of Electronic Engineering, Shantou University, China, in 2009. His research interests include intelligence engineering and industrial automation; signal processing; fiber optical sensor application; transportation monitoring and control; and environmental pollution control.

Chun-cheung Lai is a research student in the Department of Electrical Engineering, Hong Kong Polytechnic University.

Shun-yee Liu received the B.Eng. and Ph.D. degrees from the Department of Electrical Engineering, Hong Kong Polytechnic University, Kowloon.

He is now the Senior Scientific Officer with the Department of Electrical Engineering, Hong Kong Polytechnic University, and is in charge of the PolyU-KCRC Smart Railway Research Laboratory. He has been working in the field of fiber-optic sensors for 15 years and is involved in eight photonics-related patents and has published over 30 international papers.

Dr. Liu is a Chartered Engineer, a Fellow of the Society of Operations Engineers, and a member of the IET. He has won three international awards.

W. H. Chung received the B.Eng. (Hon) and Ph.D degrees form The Hong Kong Polytechnic University in 1998 and 2003, respectively.

In 2003, he joined the Photonics Research Center and the Department of Electrical Engineering, The Hong Kong Polytechnic University as a Postdoctoral Fellow and became a Research Fellow in 2005. His research focuses on fiber Bragg grating-based devices, fiber-optic sensor implementations, sensor multiplexing techniques and interrogation methods. He has published over 30 technical papers and holds four patents in the areas of fiber-optics.

Dr. Chung is a member of the Institute of Engineering and Technology (IET) and the Optical Society of America.

T. K. Ho received the B.Eng. and Ph.D. degrees in electronic and electrical engineering from the University of Birmingham, Birmingham, U.K., in 1988 and 1994, respectively.

He joined the Department of Electrical Engineering, Hong Kong Polytechnic University, in 1992 and is currently an Associate Professor. His research interests include railway signalling and operation simulation; railway maintenance and condition monitoring; railway open markets; and intelligent decision support systems.

Hwa-yaw Tam received the B.Sc. degree in 1985 and the Ph.D. degree in 1990 in electrical and electronic engineering both from the University of Manchester, Manchester, U.K.

From 1989 to 1993, he was with Hirst Research Center, GEC-Marconi, Ltd., working on wavelength-division multiplexing components and systems, and optical fiber amplifiers. His invention in low-loss fusion splicing technique for optical fiber amplifiers in 1990 is being adopted in most commercial fusion splicers. He joined the Hong Kong Polytechnic in 1993 and is currently a Chair Professor of Photonics at the Department of Electrical Engineering and Director of the Photonic Research Centre at the Hong Kong Polytechnic University. He established several state-of-the-art research facilities at PolyU, including two fiber drawing towers and several laser platforms for the fabrication of advanced fiber gratings. He has published over 450 technical papers and awarded/applied about 20 patents. He also has strong R&D collaboration with industry. His team installed a condition-monitoring system, consisting 1000 fiber sensors for Hong Kong Rails, and also a 200-sensor structural health monitoring system for the world's tallest 610-m Canton Tower, Guangzhou. His current research interests include fabrication of speciality glass and polymer fibers, fiber gratings, fiber amplifiers, optical fiber communication and fiber sensor systems.

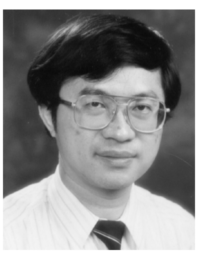

S. L. Ho received the B.Sc. and Ph.D. degrees in electrical engineering from the University of Warwick, Warwick, U.K., in 1976 and 1979, respectively.

He then joined the Hong Kong Polytechnic University in 1979 and is now a Chair Professor and Head of the Department of Electrical Engineering. Since joining the University, he has been working actively with the local industry, particularly in railway engineering. He is the holder of several patents and has published over 130 papers in leading journals, mostly in the IEEE TRANSACTIONS and IEE *Proceedings*. His main research interests include optimization, the application of finite elements in electrical machines, phantom loading of machines and optimization of electromagnetic devices.

Dr. Ho is a member of the Institution of Electrical Engineers of the U.K. and the Hong Kong Institution of Engineers.

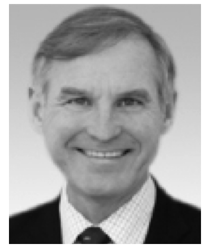

A. McCusker has served as the Operations Director with the MTR Corporation, Kowloon, Hong Kong, since December 2005. He has more than 40 years of experience in the operating, engineering, and projects fields in the defense, power, water, and rail industries. He joined the company as Operations Engineering Manager in 1987, and since then has been posted to other positions, including Operations Engineering Design Manager, Project Manager (Operations), and General Manager (Operations). He was appointed Deputy Operations Director in March 2004 and Acting Operations Director in October 2005.

Mr. McCusker is a chartered member of both the Institution of Mechanical Engineers of the United Kingdom and the Chartered Institute of Personnel and Development (U.K.). In 2007, he was awarded the prestigious Steve Maxwell Leadership Award from the Australian Asset Management Council. He is now also the Adjunct Professor at the Hong Kong Polytechnic University

J. Kam received the Ph.D. degree in structural integrity and risk management from University College, London, U.K.

He joined MTR Corporation, Ltd., Kowloon, Hong Kong, in 1995 and held several senior management positions in safety and quality, projects, engineering, operations, and international businesses, and is now the Head of Operations Engineering. Reporting directly to the Operations Director. He is responsible for the management of all railway assets in the existing network, at a total value around HK$95bn (US$12bn). His responsibilities include the assurance of system safety, reliability performance, and the management of maintenance, upgrade, and replacement programs for all railway assets.

K. Y. Lee received the M.Phil. and Eng.D. degrees from the Hong Kong Polytechnic University, Kowloon, in 1993 and 2005, respectively.

He worked in the railway industry for more than 24 years. In addition to his busy industrial work schedule, he has been involved with the research, development, and application of optical fiber Bragg grating sensor in railway engineering, including the invention that uses optical sensors for disturbance-free axle counter on track, derailment detector on wheel/rail interaction, train identification, train speed detection, and strain/stress monitoring on vehicle structure, etc. He is actively studying on harmonic and thermal performance of dc and ac traction system for nearly two decades. His current research interest is the architectural design and implementation of the FBG Sensor to build a high-performance smart railway. Currently, he is the Fleet Manager of the Mass Transit Railway Corporation looking after the frontline maintenance of the entire fleet of rolling stocks that includes trains and buses.